NASA TECHNICAL NOTE

NASA TN D-6065

NASA TN D-6065

ANALYSIS OF HEAT TRANSFER IN A BOUNDED TWO-DIMENSIONAL POROUS REGION AND APPLICATION TO A POROUS SQUARE DUCT

by Marvin E. Goldstein and Robert Siegel

Lewis Research Center
Cleveland, Ohio 44135

NATIONAL AERONAUTICS AND SPACE ADMINISTRATION • WASHINGTON, D. C. • OCTOBER 1970

1. Report No. NASA TN D-6065	2. Government Accession No.	3. Recipient's Catalog No.
4. Title and Subtitle ANALYSIS OF HEAT TRANSFER IN A BOUNDED TWO-DIMENSIONAL POROUS REGION AND APPLICATION TO A POROUS SQUARE DUCT		5. Report Date October 1970 6. Performing Organization Code
7. Author(s) Marvin E. Goldstein and Robert Siegel		8. Performing Organization Report No. E-5677 10. Work Unit No. 129-01
9. Performing Organization Name and Address Lewis Research Center National Aeronautics and Space Administration Cleveland, Ohio 44135		11. Contract or Grant No. 13. Type of Report and Period Covered Technical Note
12. Sponsoring Agency Name and Address National Aeronautics and Space Administration Washington, D. C. 20546		14. Sponsoring Agency Code
15. Supplementary Notes		

16. Abstract

Two-dimensional transpiration heat conduction is considered for a porous region bounded by four surfaces. Two opposing surfaces have no fluid flow or heat transfer across them. The other two surfaces are in contact with reservoirs at differing pressures so that fluid is forced to flow through the region. The flow exit side of the region can have an arbitrary temperature or heat flux distribution imposed along it. As a result of the boundary conditions the porous region occupies a rectangle in a suitable complex potential plane. The energy equation is transformed into the potential plane, and the general solution is found in this rectangular region. The solution can then be transformed into the geometry in the physical plane by conformal mapping. The method is illustrated by obtaining the heat-transfer characteristics of a square duct with porous walls.

17. Key Words (Suggested by Author(s)) Transpiration cooling Porous cooling Conformal mapping	18. Distribution Statement Unclassified - unlimited		
19. Security Classif. (of this report) Unclassified	20. Security Classif. (of this page) Unclassified	21. No. of Pages 48	22. Price* $3.00

*For sale by the Clearinghouse for Federal Scientific and Technical Information
Springfield, Virginia 22151

CONTENTS

ANALYSIS OF HEAT TRANSFER IN A BOUNDED TWO-DIMENSIONAL POROUS REGION AND APPLICATION TO A POROUS SQUARE DUCT

by Marvin E. Goldstein and Robert Siegel

Lewis Research Center

SUMMARY

A finite two-dimensional permeable porous region is considered bounded by four surfaces. Two of the opposing surfaces have no fluid flow or heat transfer across them and are consequently along the direction of the fluid and heat flows. The other two surfaces are each in contact with a reservoir at a different constant pressure, and this produces a flow toward the low pressure reservoir. The flow is assumed to be governed by Darcy's law, and hence, the pressure acts as a velocity potential. As a result of the boundary conditions the porous region occupies a rectangular region in a complex potential plane. The energy equation for the temperature distribution in the medium is shown to be transformed into a separable equation when its independent variables are changed to the coordinates of the potential plane. The general solution is obtained in the potential plane for the cases where the side of the porous material at which the flow exits is either maintained at an arbitrary temperature or has an arbitrary imposed heat flux. Conformal mapping is then used to relate the solution to the physical geometry. The method is illustrated by obtaining the heat-transfer characteristics of a square duct with porous walls of finite thickness.

INTRODUCTION

A method for extending the use of a metallic structural material to higher temperature applications is to provide transpiration cooling. The metal is made in a porous form, and coolant is forced through it from a reservoir toward the boundary exposed to the high temperature source. Some possible applications are for cooling turbine blades, rocket nozzles, arc electrodes, and portions of surfaces during either high speed flight or reentry into the Earth's atmosphere.

The energy equation governing the temperature distribution in the permeable porous

material contains the velocity distribution. The velocity is generally a complicated function of position, which makes it difficult to solve the energy equation analytically. The solutions in the literature have consequently been limited to one-dimensional situations. However, in many applications, the geometries are two- or three-dimensional. Solutions can be obtained numerically, but it would be desirable to have some analytical results to check numerical and approximate procedures. In addition, formulas derived from analytical solutions can be used for calculating results at the porous boundaries without obtaining detailed calculations for the interior of the region as in a numerical solution. This is convenient for coupling the heat transfer in the porous medium into the overall heat transfer system such as coupling it with an external thermal boundary layer. Analytical results are also useful in evaluating the importance of the governing parameters and in helping to determine conditions when two- or three-dimensional effects become significant so that a locally one-dimensional solution will not apply.

For these reasons the present authors devised in reference 1 an analytical method for obtaining the heat-transfer behavior in a two-dimensional porous medium. The theory was developed for a porous wall of arbitrarily varying thickness but of infinite length. The purpose of the present report is to extend the theory to finite two-dimensional regions. The example used to illustrate the general solution that is obtained is the heat transfer in a square duct with porous walls of a finite thickness.

The following is a brief outline of the analytical method derived in reference 1 that will be further developed and applied herein. As stated in reference 1, it will be assumed that the fluid and solid matrix are locally in good thermal contact so that the local fluid and solid matrix temperatures are equal. As a consequence, a single energy equation can be written that includes the heat transport by conduction in the matrix as well as by coolant convection.

The velocity in the convective term of the energy equation is a function of position and is proportional to the local pressure gradient for the slow viscous flow often encountered in porous media. The pressure can therefore be regarded as the velocity potential. The equations governing the problem are transformed into a potential plane. Since two boundaries of the porous medium are at constant pressure, these become parallel lines in the potential plane. The other two boundaries have no flow across them and, hence, are perpendicular to the constant potential boundaries. Thus, in the potential plane the porous region becomes a rectangle.

Since the geometry in the potential plane is simply a rectangle regardless of the physical shape of the porous material, a solution in this region of the potential plane will apply to all geometries. An important factor is that, when the energy equation is transformed into the potential plane, it becomes a separable equation, and hence, the general solution can be obtained for the rectangular region. This solution can then be transformed into specific physical geometries by conformal mapping. If the geometry is too

complicated to map analytically, the mapping can be performed numerically; one technique for this is given in reference 2.

SYMBOLS

A	half-width of outside of square duct divided by wall thickness
a	half-width of outside of square duct
$\tilde{B}_n$	coefficient defined following eq. (48)
C_p	specific heat of fluid
F	incomplete elliptic integral of first kind
G	function in specified heat flux distribution
H	function in specified temperature distribution
h_r	reference length in porous material
K	complete elliptic integral of first kind; $K'(k) = K\left(\sqrt{1 - k^2}\right)$
k_m	thermal conductivity of porous region
k_1, k_2	quantities defined in eq. (A8)
L_s	dimensionless coordinate along boundary S, l_s/h_r
l_s	coordinate along boundary s measured from left side
M	heat flux parameter $(q_2 - q_1)/q_1$
N	temperature parameter $(t_2 - t_1)/(t_1 - t_\infty)$
$\hat{n}$	unit outward normal vector
p	pressure
q	heat flux
S	bounding surfaces of porous region in dimensionless coordinate system
s	bounding surfaces of porous region
T	dimensionless temperature defined in eqs. (11) and (12)
t	temperature
$\vec{U}$	dimensionless velocity, $\frac{\mu}{\kappa} \frac{h_r}{p_o - p_s} \vec{u}$
$\vec{u}$	velocity

u	intermediate mapping plane, $\alpha + i\beta$
V	dimensionless velocity component in Y-direction
v	velocity component in y-direction
W	complex potential, $\psi + i\varphi$
X, Y	dimensionless coordinates, x/h_r and y/h_r
x, y	rectangular coordinates
Z	dimensionless physical plane, $X + iY$
α	real part of u-plane
β	separation constant in solution for Θ; imaginary part of u-plane
γ_n	quantity defined in eq. (48)
Δ	nondimensionalizing quantity defined by eq. (12)
η	imaginary part of ω
Θ	variable defined in eq. (38)
κ	permeability of porous material
λ	parameter, $\frac{\rho C_p}{2k_m} \frac{\kappa(p_o - p_s)}{\mu}$
μ	fluid viscosity
ξ	real part of ω
ρ	fluid density
Φ	function of φ in solution for Θ
φ	potential $(p_o - p)/(p_o - p_s)$, imaginary part of W
Ψ	function of ψ in solution for Θ
ψ	real part of W
Ω	quantity defined in eq. (A15)
ω	intermediate mapping plane, $\xi + i\eta$
$\tilde{\nabla}$	dimensionless gradient defined in eq. (18)

Subscripts:

l	at left boundary
o	at lower boundary

r at right boundary

s at upper boundary

1, 2 values on upper boundary at left and right sides

∞ coolant reservoir

GENERAL ANALYSIS OF TWO-DIMENSIONAL POROUS COOLED REGION

Governing Equations

Consider the two-dimensional porous region with effective thermal conductivity k_m (based on the entire cross sectional area) and permeability κ shown in figure 1(a). The lower surface of the region whose unit outward-drawn normal is $\hat{n}_o$ is denoted by s_o and the upper surface of the region whose unit outward-drawn normal is $\hat{n}_s$ is denoted by s. The left and right surfaces of the region whose unit outward-drawn normals are

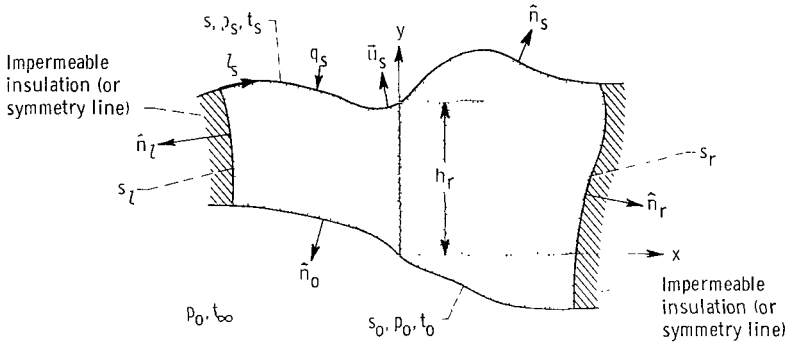

(a) Cross section in physical plane.

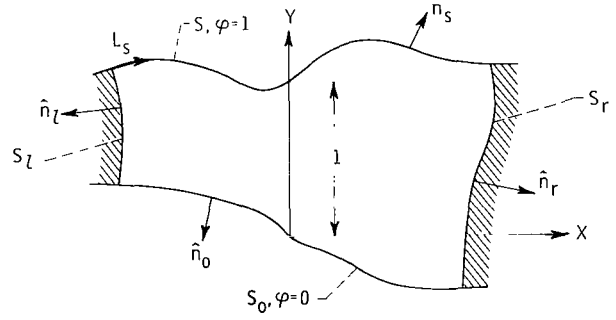

(b) Dimensionless physical plane.

Figure 1. - Two-dimensional porous region with no fluid or heat flow through two opposite sides.

$\hat{n}_\ell$ and $\hat{n}_r$, respectively, are denoted by s_ℓ and s_r, respectively. There is a fluid with constant density ρ, constant heat capacity C_p, and constant viscosity μ which is flowing through the region. Assume that the thermal conductivity of the fluid is very small compared with k_m and that the pore size is so small that Darcy's law holds. Let $\vec{u}$ denote the Darcy velocity (local volume flow divided by entire cross section rather than by open area) of the fluid. We suppose that no changes occur in the direction perpendicular to the x,y-plane so the situation is two-dimensional.

Below the porous region (see fig. 1(a)) there is a reservoir which is maintained at constant pressure and temperature p_o and t_∞, respectively. There is no heat or mass flow across the surfaces s_ℓ and s_r. The pressure of the fluid above the wall is constant and equal to p_s. We suppose that $p_o > p_s$. Then the fluid flows from the reservoir through the porous region and out through the top surface. Since p_o and p_s are both constant, the fluid velocity at both the upper and lower region surfaces will be in a direction perpendicular to these surfaces.

If the thermal communication between the fluid and the matrix is sufficiently good, the local fluid temperature will be approximately equal to the local solid matrix temperature. We denote this common temperature by t. When these assumptions are made, the heat and mass flow within the porous material are governed by the equations given in reference 1. Thus,

$$k_m \nabla^2 t - \rho C_p \vec{u} \cdot \nabla t = 0 \tag{1}$$

$$\vec{u} = -\frac{K}{\mu} \nabla p \tag{2}$$

$$\nabla \cdot \vec{u} = 0 \tag{3}$$

Boundary Conditions

As the fluid in the reservoir approaches the porous region, the fluid temperature will rise from the reservoir temperature t_∞ to the region surface temperature t_o which is an unknown variable along s_o. Since the thermal conductivity of the fluid is assumed to be much less than the thermal conductivity of the matrix material, the thickness of the fluid layer over which this temperature rise takes place is very small compared with the porous region thickness provided the flow is not very small. We can, therefore, assume that the liquid layer is locally one-dimensional. Since the velocity is perpendicular to s_o, there is no flow along this thermal layer. Hence, applying an energy balance to the thermal layer shows that

$$\left.\begin{aligned} k_m \hat{n}_o \cdot \nabla t &= \rho C_p (t - t_\infty) \hat{n}_o \cdot \vec{u} \\ p &= p_o \end{aligned}\right\} \quad \text{for } (x, y) \epsilon s_o \tag{4}$$

Since there is no flow of heat or mass across the side surfaces s_l and s_r, the normal derivative of both the pressure and the temperature must vanish at these surfaces. Hence,

$$\left.\begin{aligned} \hat{n}_l \cdot \nabla t &= 0 \\ \hat{n}_l \cdot \nabla p &= 0 \end{aligned}\right\} \quad \text{for } (x, y) \epsilon s_l \tag{5}$$

$$\left.\begin{aligned} \hat{n}_r \cdot \nabla t &= 0 \\ \hat{n}_r \cdot \nabla p &= 0 \end{aligned}\right\} \quad \text{for } (x, y) \epsilon s_r \tag{6}$$

We shall consider two different types of thermal boundary conditions for the upper surface s. First, we shall suppose that its surface temperature is specified so that it varies along the surface from a temperature t_1 at the left end to a temperature t_2 at the right end. Let l_s be the distance measured along the upper surface from its left end. Then for this case the boundary conditions on the upper surface of the region are

$$\left.\begin{aligned} t = t_s &= t_1 + (t_2 - t_1) H\left(\frac{l_s}{h_r}\right) \\ p &= p_s \end{aligned}\right\} \quad \text{for } (x, y) \epsilon s \tag{7a}$$

where H is a given function equal to zero at $(l_s/h_r) = 0$ and equal to 1 when (l_s/h_r) is a maximum. The constant h_r is an appropriate reference length.

We shall also consider the case where the heat flux into the wall is specified along the upper surface and it varies from a value of q_1 at the left end to a value of q_2 at the right end. Under these conditions the boundary conditions on the upper surface become

$$\left.\begin{aligned} k_m \hat{n}_s \cdot \nabla t = q_s &= q_1 + (q_2 - q_1) G\left(\frac{\ell_s}{h_r}\right) \\ p &= p_s \end{aligned}\right\} \quad \text{for } (x,y) \epsilon s \tag{7b}$$

where G is a given function which is equal to zero at ℓ_s/h_r equal to zero, and equal to 1 when ℓ_s/h_r is a maximum.

Equations (1) to (3) together with either boundary conditions (4) to (6) and (7a) or alternatively the boundary conditions (4) to (6) and (7b) completely determine the solution to the heat transfer and flow problems within the porous wall.

Dimensionless Equations

It is now convenient to introduce the following dimensionless quantities:

$$\lambda \equiv \frac{\rho C_p}{2k_m} \frac{\kappa(p_o - p_s)}{\mu} \tag{8}$$

$$N = \frac{t_2 - t_1}{t_1 - t_\infty} \tag{9}$$

$$M = \frac{q_2 - q_1}{q_1} \tag{10}$$

$$
\left.
\begin{aligned}
X &= \frac{x}{h_r} \\
Y &= \frac{y}{h_r} \\
L_s &= \frac{\ell_s}{h_r} \\
\varphi &= \frac{p_o - p}{p_o - p_s} \\
\vec{U} &= \frac{\mu}{\kappa (p_o - p_s)} \frac{h_r}{} \vec{u} \\
T &= \frac{t - t_\infty}{\Delta}
\end{aligned}
\right\} \tag{11}
$$

where

$$
\Delta \equiv \left\{
\begin{aligned}
&(t_1 - t_\infty) \text{ if boundary condition (7a) applies} \\
&\frac{q_1 h_r}{k_m} \text{ if boundary condition (7b) applies}
\end{aligned}
\right\} \tag{12}
$$

Upon substituting these definitions into equations (1) to (3) and boundary conditions (4) to (7b), we obtain

$$
\left.
\begin{aligned}
\tilde{\nabla}^2 T - 2\lambda \vec{U} \cdot \tilde{\nabla} T &= 0 \\
\vec{U} &= \tilde{\nabla} \varphi \\
\tilde{\nabla} \cdot \vec{U} &= 0
\end{aligned}
\right\} \tag{13}
$$

$$\left.\begin{aligned} \hat{n}_o \cdot \tilde{\nabla} T &= 2\lambda \hat{n}_o \cdot \vec{U} T \\ \varphi &= 0 \end{aligned}\right\} \quad \text{for } (X, Y) \epsilon S_o \tag{14}$$

$$\left.\begin{aligned} \hat{n}_\ell \cdot \tilde{\nabla} T &= 0 \\ \hat{n}_\ell \cdot \tilde{\nabla} \varphi &= 0 \end{aligned}\right\} \quad \text{for } (X, Y) \epsilon S_\ell \tag{15}$$

$$\left.\begin{aligned} \hat{n}_r \cdot \tilde{\nabla} T &= 0 \\ \hat{n}_r \cdot \tilde{\nabla} \varphi &= 0 \end{aligned}\right\} \quad \text{for } (X, Y) \epsilon S_r \tag{16}$$

$$\left.\begin{aligned} T &= 1 + NH(L_s) \\ \varphi &= 1 \end{aligned}\right\} \quad \text{for } (X, Y) \epsilon S \tag{17a}$$

or

$$\left.\begin{aligned} \hat{n}_s \cdot \tilde{\nabla} T &= 1 + MG(L_s) \\ \varphi &= 1 \end{aligned}\right\} \quad \text{for } (X, Y) \epsilon S \tag{17b}$$

where

$$\tilde{\nabla} \equiv \hat{i} \frac{\partial}{\partial X} + \hat{j} \frac{\partial}{\partial Y} \tag{18}$$

and the porous region in dimensionless coordinates is shown in figure 1(b).

The second equation (13) can be used to eliminate $\vec{U}$ in the other two equations (13). Thus,

$$\tilde{\nabla}^2 T - 2\lambda \tilde{\nabla} \varphi \cdot \tilde{\nabla} T = 0 \tag{19}$$

and

$$\tilde{\nabla}^2 \varphi = 0 \tag{20}$$

Since φ is constant on both S_o and S, it is clear that

$$\hat{n}_o = - \frac{\tilde{\nabla}\varphi}{|\tilde{\nabla}\varphi|} \qquad \text{for } (X, Y) \epsilon S_o \tag{21a}$$

and

$$\hat{n}_s = \frac{\tilde{\nabla}\varphi}{|\tilde{\nabla}\varphi|} \qquad \text{for } (X, Y) \epsilon S \tag{21b}$$

Using these results together with the second equation (13) in the boundary conditions (14) and (17b), we obtain

$$\left.\begin{aligned} \tilde{\nabla}\varphi \cdot \tilde{\nabla}T &= 2\lambda T |\tilde{\nabla}\varphi|^2 \\ \varphi &= 0 \end{aligned}\right\} \qquad \text{for } (X, Y) \epsilon S_o \tag{22a}$$

and

$$\left.\begin{aligned} \tilde{\nabla}\varphi \cdot \tilde{\nabla}T &= |\tilde{\nabla}\varphi| \left[1 + MG(L_s)\right] \\ \varphi &= 1 \end{aligned}\right\} \qquad \text{for } (X, Y) \epsilon S \tag{22b}$$

Porous Region in Potential Plane

Since equation (20) shows that φ satisfies Laplace's equation, there must exist a harmonic function ψ and an analytic function W of the complex variable

$$Z = X + iY \tag{23}$$

such that

$$W = \psi + i\varphi \tag{24}$$

Physically the change in ψ between any two points is proportional to the volume flow of liquid crossing any curve joining those two points. Hence, since there is no flow across either surface S_l or S_r, the function ψ must be constant on both of these surfaces. Since W is determined only to within an arbitrary constant, we can always arrange matters so that

$$\psi = 0 \qquad \text{for } (X, Y) \epsilon S_l \tag{25}$$

We shall denote the constant value of ψ on S_r by ψ_r. Thus,

$$\mathcal{I}m\, W = 0 \qquad \text{for } Z \epsilon S_o$$

$$\mathcal{I}m\, W = 1 \qquad \text{for } Z \epsilon S$$

$$\mathcal{R}e\, W = 0 \qquad \text{for } Z \epsilon S_l$$

$$\mathcal{R}e\, W = \psi_r \qquad \text{for } Z \epsilon S_r$$

This shows that the mapping

$$Z \rightarrow W$$

transforms the region occupied by the porous material in the dimensionless physical plane (Z-plane) shown in figure 1(b) into the rectangular region in the W-plane shown

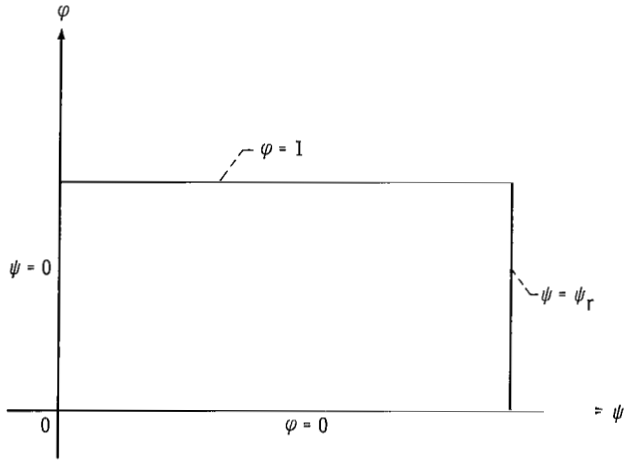

Figure 2. - Porous region in complex potential plane $W = \psi + i\varphi$.

in figure 2. The boundaries S_o and S in the physical plane are transformed into the lines $\varphi = 0$ and $\varphi = 1$, respectively, in the W-plane, and the boundaries S_l and S_r in the physical plane are transformed into the lines $\psi = 0$ and $\psi = \psi_r$, respectively, in the W-plane. The mapping $Z \rightarrow W$ can be found by using the techniques of conformal mapping once the shape of the porous wall in the physical plane is specified. This gives the solution to the boundary value problem for the mass flow. (An example for a specific wall geometry will be worked out subsequently.)

Since ψ is constant on both S_l and S_r, it is clear that

$$\hat{n}_l = -\frac{\tilde{\nabla}\psi}{|\tilde{\nabla}\psi|} \qquad \text{for } (X, Y) \epsilon S_l$$

$$\hat{n}_r = \frac{\tilde{\nabla}\psi}{|\tilde{\nabla}\psi|} \qquad \text{for } (X, Y) \epsilon S_r$$

Using these results together with equation (25) in the boundary conditions (15) and (16), we obtain

$$\left.\begin{aligned} \tilde{\nabla}\psi \cdot \tilde{\nabla}T = 0 \\ \psi = 0 \end{aligned}\right\} \qquad \text{for } (X, Y) \epsilon S_l \tag{26}$$

and

$$\left.\begin{aligned} \tilde{\nabla}\psi \cdot \tilde{\nabla}T = 0 \\ \psi = \psi_r \end{aligned}\right\} \qquad \text{for } (X, Y) \epsilon S_r \tag{27}$$

Transformation of Boundary Value Problem Into Potential Plane

The boundary value problem for the temperature in the physical plane can be solved if we use the Boussinesq transform (ref. 3) to transform it into a boundary value problem in the W-plane. Thus, the independent variables X and Y in equation (19) and its boundary conditions will be changed to the variables φ and ψ, and the resulting boundary value problem will be solved in the rectangular region in the W-plane shown in figure 2. Once this solution which gives T as a function of φ and ψ has been found, the mapping $W \rightarrow Z$ (which is completely determined once the geometry of the region in the physical plane is specified) can be inverted to give Z as a function of φ and ψ.

Thus, T will be known parametrically (in terms of the parameters φ and ψ) as a function of X and Y. This will complete the solution to the problem.

Apropos of these remarks, recall that (ref. 4)

$$\widetilde{\nabla}^2 T = \left(\frac{\partial^2 T}{\partial \psi^2} + \frac{\partial^2 T}{\partial \varphi^2} \right) \left| \frac{dW}{dZ} \right|^2 \tag{28}$$

and

$$\left| \widetilde{\nabla} \varphi \right| = \left| \frac{dW}{dZ} \right| \tag{29}$$

Notice that

$$\frac{dW}{dZ} = \frac{dW}{dZ} \left(\frac{dZ}{dW} \frac{dW}{dZ} \right)^* = \left| \frac{dW}{dZ} \right|^2 \left(\frac{dZ}{dW} \right)^*$$

Hence, upon taking real and imaginary parts, we find

$$\frac{\partial \varphi}{\partial X} = \left| \frac{dW}{dZ} \right|^2 \frac{\partial X}{\partial \varphi}$$

$$\frac{\partial \varphi}{\partial Y} = \left| \frac{dW}{dZ} \right|^2 \frac{\partial Y}{\partial \varphi}$$

and

$$\frac{\partial \psi}{\partial X} = \left| \frac{dW}{dZ} \right|^2 \frac{\partial X}{\partial \psi}$$

$$\frac{\partial \psi}{\partial Y} = \left| \frac{dW}{dZ} \right|^2 \frac{\partial Y}{\partial \psi}$$

This shows that

$$\tilde{\nabla}\varphi \cdot \tilde{\nabla}T = \left(\frac{\partial T}{\partial X}\frac{\partial X}{\partial \varphi} + \frac{\partial T}{\partial Y}\frac{\partial Y}{\partial \varphi}\right)\left|\frac{dW}{dZ}\right|^2 = \frac{\partial T}{\partial \varphi}\left|\frac{dW}{dZ}\right|^2 \tag{30}$$

and

$$\tilde{\nabla}\psi \cdot \tilde{\nabla}T = \frac{\partial T}{\partial \psi}\left|\frac{dW}{dZ}\right|^2 \tag{31}$$

Finally, notice that since φ is constant on S, the distance L_s along S is a function of ψ only. (This functional relation is known once the mapping $W \rightarrow Z$ which solves the flow problem is known.) Thus,

$$L_s(X, Y) = L_s(\psi) \qquad \text{for } (X, Y) \in S \tag{32}$$

Now, using equations (28) to (32) in equation (19) and the boundary conditions (22a), (26), (27), (17a), and (22b) yields

$$\frac{\partial^2 T}{\partial \psi^2} + \frac{\partial^2 T}{\partial \varphi^2} - 2\lambda \frac{\partial T}{\partial \varphi} = 0 \tag{33}$$

$$\frac{\partial T}{\partial \varphi} - 2\lambda T = 0 \qquad \text{for } \varphi = 0 \tag{34}$$

$$\frac{\partial T}{\partial \psi} = 0 \qquad \text{for } \psi = 0 \tag{35}$$

$$\frac{\partial T}{\partial \psi} = 0 \qquad \text{for } \psi = \psi_r \tag{36}$$

$$T = 1 + NH(L_s(\psi)) \qquad \text{for } \varphi = 1 \tag{37a}$$

or

$$\frac{\partial T}{\partial \varphi} = \left|\frac{dZ}{dW}\right| \left[1 + MG(L_s(\psi))\right] \qquad \text{for } \varphi = 1 \tag{37b}$$

It is convenient at this stage to introduce the new dependent variable Θ defined by

$$\Theta \equiv e^{\lambda(1-\varphi)}T = e^{\lambda(1-\varphi)}\frac{(t - t_\infty)}{\Delta} \tag{38}$$

In terms of this new variable equations (33) to (37b) become

$$\frac{\partial^2\Theta}{\partial\psi^2} + \frac{\partial^2\Theta}{\partial\varphi^2} - \lambda^2\Theta = 0 \tag{39}$$

$$\frac{\partial\Theta}{\partial\varphi} = \lambda\Theta \qquad \text{at} \quad \varphi = 0 \tag{40}$$

$$\frac{\partial\Theta}{\partial\psi} = 0 \qquad \text{at} \quad \psi = 0 \tag{41}$$

$$\frac{\partial\Theta}{\partial\psi} = 0 \qquad \text{at} \quad \psi = \psi_r \tag{42}$$

$$\Theta = 1 + NH(L_s(\psi)) \qquad \text{at} \quad \varphi = 1 \tag{43a}$$

or

$$\frac{\partial\Theta}{\partial\varphi} + \lambda\Theta = \left|\frac{dZ}{dW}\right| \left[1 + MG(L_s(\psi))\right] \qquad \text{at} \quad \varphi = 1 \tag{43b}$$

Equation (39) together with the boundary conditions (40) to (43a) (or alternatively (40) to (42) and (43b)) constitute a boundary value problem for Θ in the rectangular region of the W-plane shown in figure 2 which completely determines Θ (and therefore T) as a function of φ and ψ. Notice that the particular relation between Z and W (which depends only upon the geometry of the porous wall in the physical plane enters only through the boundary condition (43a) (or alternatively (43b)) since L_s and $|dZ/dW|$ must be known functions of ψ in order to completely determine these boundary conditions. It is, however, possible to solve these boundary value problems for arbitrary L_s and $|dZ/dW|$ (as well as arbitrary H and G), and so the particular geometry and boundary conditions can be substituted into the general formulas once this general solution has been obtained.

General Solution of Boundary Value Problem in W-Plane

The boundary value problem posed by equation (39) and the boundary conditions (40) to (43a) (or alternatively the boundary conditions (40) to (42) and (43b)) can easily be solved by the method of separation of variables. To this end we substitute a trial solution of the form

$$\Theta(\psi, \varphi) = \Psi(\psi)\Phi(\varphi) \tag{44}$$

into equation (39) and obtain

$$\frac{\Psi''}{\Psi} + \frac{\Phi''}{\Phi} = \lambda^2$$

This implies that there exists a constant β such that

$$\frac{\Psi''}{\Psi} = -\beta^2$$

and

$$\frac{\Phi''}{\Phi} = \lambda^2 + \beta^2$$

Hence

$$\Phi = c_1 e^{\sqrt{\lambda^2+\beta^2}\varphi} + c_2 e^{-\sqrt{\lambda^2+\beta^2}\varphi} \tag{45}$$

$$\Psi = c_3 \sin \beta\psi + c_4 \cos \beta\psi \tag{46}$$

where c_1 to c_4 are arbitrary constants of integration.

Upon substituting equations (44) to (46) into the boundary condition (40), we find that this boundary condition will be automatically satisfied if

$$c_1\sqrt{\lambda^2 + \beta^2} - c_2\sqrt{\lambda^2 + \beta^2} = \lambda(c_1 + c_2)$$

or

$$c_2 = c_1 \frac{\sqrt{\lambda^2 + \beta^2} - \lambda}{\sqrt{\lambda^2 + \beta^2} + \lambda}$$

Using this expression in equation (45) gives

$$\Phi = \frac{2c_1}{\sqrt{\lambda^2 + \beta^2} + \lambda} \left[\lambda \sinh\left(\sqrt{\lambda^2 + \beta^2}\, \varphi\right) + \sqrt{\lambda^2 + \beta^2} \cosh\left(\sqrt{\lambda^2 + \beta^2}\, \varphi\right) \right]$$

The boundary condition (41) will be automatically satisfied if we put

$$c_3 = 0$$

and the boundary condition (42) will be satisfied if we set

$$\beta = \frac{n\pi}{\psi_r} \qquad \text{for } n = 0,\ 1,\ 2,\ \ldots$$

Hence, the solution to both boundary value problems must be of the form

$$\Theta = \sum_{n=0}^{\infty} C_n \left[\lambda \sinh(\gamma_n \varphi) + \gamma_n \cosh(\gamma_n \varphi) \right] \cos \frac{n\pi}{\psi_r} \psi \tag{47}$$

where

$$\gamma_n \equiv \sqrt{\lambda^2 + \left(\frac{n\pi}{\psi_r}\right)^2} \qquad \text{for } n = 0,\ 1,\ 2,\ \ldots \tag{48}$$

and the constants C_n can be determined so that either the boundary condition (43a) or the boundary condition (43b) is satisfied.

Solution to Boundary Value Problem for Specified Temperature

First suppose that the boundary condition (43a) applies. Put

$$\tilde{B}_n = C_n\left[\lambda \sinh \gamma_n + \gamma_n \cosh \gamma_n\right] \qquad \text{for } n = 0,\ 1,\ 2,\ \ldots$$

Then equation (47) becomes

$$\Theta = \sum_{n=0}^{\infty} \tilde{B}_n \left[\frac{\lambda \sinh \gamma_n\varphi + \gamma_n \cosh \gamma_n\varphi}{\lambda \sinh \gamma_n + \gamma_n \cosh \gamma_n}\right] \cos\left(\frac{n\pi}{\psi_r}\psi\right) \tag{49}$$

Substituting this result into the boundary condition (43a) yields

$$1 + NH(L_s(\psi)) = \sum_{n=0}^{\infty} \tilde{B}_n \cos\left(\frac{n\pi}{\psi_r}\psi\right)$$

Hence, the theory of Fourier series shows that

$$\tilde{B}_0 = \frac{1}{\psi_r}\int_0^{\psi_r} \left[1 + NH(L_s(\psi))\right] d\psi$$

$$\tilde{B}_n = \frac{2}{\psi_r}\int_0^{\psi_r} \left[1 + NH(L_s(\psi))\right] \cos\left(\frac{n\pi}{\psi_r}\psi\right) d\psi \qquad \text{for } n = 1,\ 2,\ 3,\ \ldots$$

or

$$\left.\begin{aligned} \tilde{B}_0 &= 1 + NB_0 \\ \tilde{B}_n &= NB_n \qquad \text{for } n = 1,\ 2,\ \ldots \end{aligned}\right\} \tag{50}$$

where

$$B_0 \equiv \frac{1}{\psi_r} \int_0^{\psi_r} H(L_s(\psi))d\psi$$

$$B_n \equiv \frac{2}{\psi_r} \int_0^{\psi_r} H(L_s(\psi))\cos\left(\frac{n\pi\psi}{\psi_r}\right)d\psi \qquad \text{for } n = 1, 2, \ldots \tag{51}$$

Substituting equation (50) into equation (49) yields

$$\Theta = e^{\lambda(\varphi-1)} + N \sum_{n=0}^{\infty} B_n \left[\frac{\lambda \sinh \gamma_n\varphi + \gamma_n \cosh \gamma_n\varphi}{\lambda \sinh \gamma_n + \gamma_n \cosh \gamma_n}\right] \cos\left(\frac{n\pi\psi}{\psi_r}\right) \tag{52}$$

Thus, equation (52) with the constant B_n defined in terms of the dimensionless temperature distribution H by equation (51) is the solution to the boundary value problem.

In this case, it is of interest for practical applications to have an expression for the conduction heat flux q_s flowing into the surface s. This can be obtained from

$$q_s = k_m \hat{n}_s \cdot \nabla t \qquad \text{for } (x, y) \epsilon s$$

Hence, for $(X, Y) \epsilon S$ (by the use of eqs. (21b), (29), and (30))

$$\frac{q_s h_r}{k_m(t_1 - t_\infty)} = \hat{n}_s \cdot \tilde{\nabla} T = \frac{\tilde{\nabla}\varphi \cdot \tilde{\nabla} T}{|\tilde{\nabla}\varphi|} = \left|\frac{dW}{dZ}\right| \frac{\partial T}{\partial \varphi}$$

By using equation (38) and the fact that $\varphi = 1$ on the boundary s, we find

$$\frac{q_s h_r}{k_m(t_1 - t_\infty)} = \left|\frac{dW}{dZ}\right| \left(\frac{\partial \Theta}{\partial \varphi} + \lambda\Theta\right)\Bigg|_{\varphi=1}$$

Upon substituting equations (43a) and (52) into this expression, we obtain

$$\frac{q_s h_r}{k_m(t_1 - t_\infty)} = \left|\frac{dW}{dZ}\right|_{\varphi=1} \left\{ 2\lambda + \lambda N H(L_s(\psi)) + N \sum_{n=0}^{\infty} B_n \gamma_n \left[\frac{\lambda \cosh \gamma_n + \gamma_n \sinh \gamma_n}{\lambda \sinh \gamma_n + \gamma_n \cosh \gamma_n} \right] \cos\left(\frac{n\pi}{\psi_r} \psi \right) \right\} \tag{53}$$

Solution to Boundary Value Problem for Specified Heat Flux

Now suppose that the boundary condition (43b) applies. Put

$$E_n = C_n \left[\left(\lambda^2 + \gamma_n^2 \right) \sinh \gamma_n + 2\lambda \gamma_n \cosh \gamma_n \right] \qquad \text{for } n = 0, 1, 2, \ldots$$

Then equation (47) becomes

$$\Theta = \sum_{n=0}^{\infty} E_n \left[\frac{\lambda \sinh \gamma_n \varphi + \gamma_n \cosh \gamma_n \varphi}{\left(\lambda^2 + \gamma_n^2 \right) \sinh \gamma_n + 2\lambda \gamma_n \cosh \gamma_n} \right] \cos\left(\frac{n\pi\psi}{\psi_r} \right) \tag{54}$$

Substituting this result into the boundary condition (43b) yields

$$\left|\frac{dZ}{dW}\right|_{\varphi=1} \left[1 + MG(L_s(\psi)) \right] = \sum_{n=0}^{\infty} E_n \cos\left(\frac{n\pi}{\psi_r} \psi \right)$$

Hence, the theory of Fourier series shows that

$$\left.\begin{aligned} E_0 &= \frac{1}{\psi_r}\int_0^{\psi_r}\left|\frac{dZ}{dW}\right|_{\varphi=1}\left[1 + MG(L_s(\psi))\right]d\psi \\ E_n &= \frac{2}{\psi_r}\int_0^{\psi_r}\left|\frac{dZ}{dW}\right|_{\varphi=1}\left[1 + MG(L_s(\psi))\right]\cos\left(\frac{n\pi\psi}{\psi_r}\right)d\psi \qquad \text{for } n = 1, 2, 3 \ldots \end{aligned}\right\} \quad (55)$$

Thus, equation (54), with the constants E_n defined by equation (55) in terms of the dimensionless heat flux distribution G and the term $\left|dZ/dW\right|_{\varphi=1}$ (this will be shown by eq. (64) to be the reciprocal of the surface velocity), is the solution to this boundary value problem. In particular, the upper surface temperature distribution is obtained by using equations (54) and (38) evaluated at $\varphi = 1$ to obtain

$$\frac{(t_s - t_\infty)k_m}{h_r q_s} = \sum_{n=0}^{\infty} E_n\left[\frac{\lambda \sinh \gamma_n + \gamma_n \cosh \gamma_n}{\left(\lambda^2 + \gamma_n^2\right)\sinh \gamma_n + 2\lambda\gamma_n \cosh \gamma_n}\right]\cos\left(\frac{n\pi\psi}{\psi_r}\right) \quad (56)$$

HEAT-TRANSFER CHARACTERISTICS FOR A POROUS SQUARE DUCT

To illustrate the use of the general solution, heat-transfer results will be obtained for a square duct with porous walls as shown in figure 3(a). Cooling fluid is flowing from an outer reservoir at temperature t_∞ through the duct wall and into the duct interior. The thickness of the duct wall is used as the reference dimension h_r so that a quarter of the duct appears in the dimensionless physical plane as shown in figure 3(b).

Conformal Mapping Relations Between Physical (Z) and Potential (W) Planes

The general solution was obtained in the W-plane, and hence, the heat-transfer quantities along the duct interior boundary are given in terms of the variable ψ. The function L_s of ψ which relates the physical distance in the X, Y-plane to ψ must be determined. Also the quantity $\left|dW/dZ\right|_{\varphi=1}$ must be found as a function of ψ since it appears in the general solution. These relations can be obtained from the mapping function $Z \rightarrow W$ between the regions in figures 3(b) and 4(a). This mapping has been carried

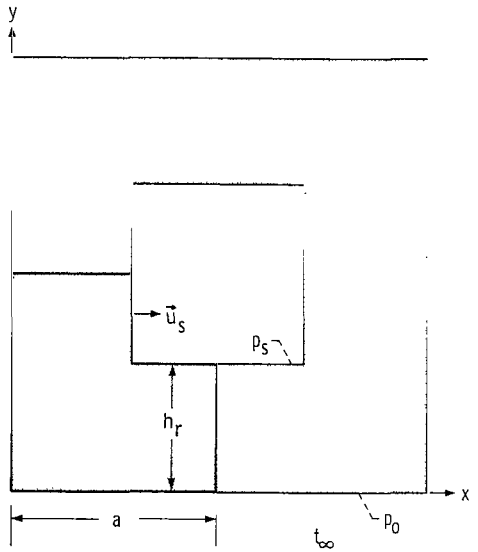

(a) Duct cross section in physical plane.

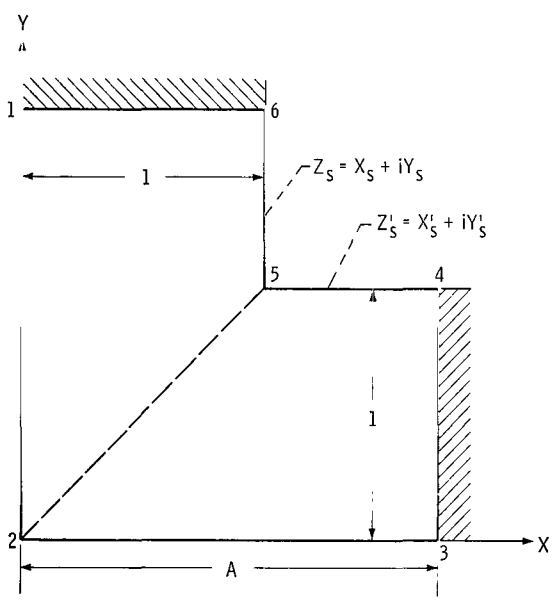

(b) One-quarter of duct in dimensionless physical plane Z = X + iY.

Figure 3. - Porous cooled square duct.

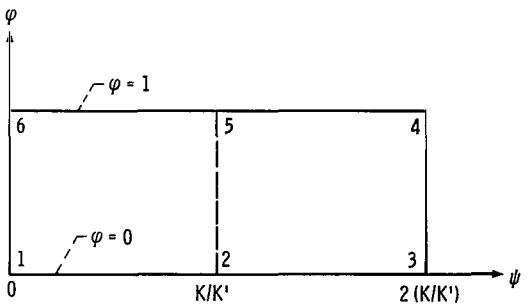

(a) Rectangle in potential plane $W = \psi + i\varphi$.

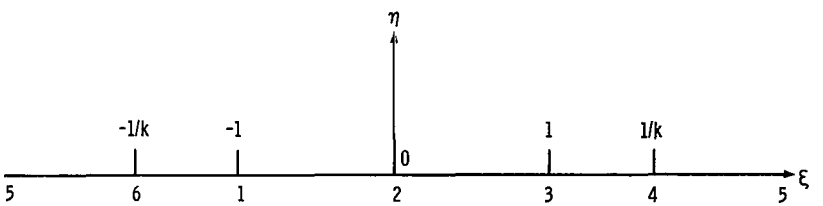

(b) Intermediate ω-plane $\omega = \xi + i\eta$.

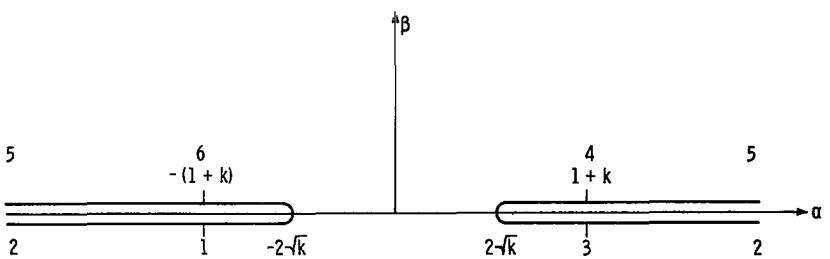

(c) Intermediate u-plane $u = \alpha + i\beta$.

Figure 4. - Mapping of quarter of duct into potential and intermediate planes.

out in appendix A. The relations between ψ and X, Y along the duct interior boundary are given by equations (A16).

The term $\left|dW/dZ\right|_{\varphi=1}$ can be found by using the relation

$$\frac{dW}{dZ} = \frac{dW}{d\omega}\frac{d\omega}{dZ} \tag{57}$$

It follows from equation (A1) of appendix A that

$$WK' - K = \int_0^{\omega} \frac{d\omega}{\sqrt{(1 - \omega^2)(1 - k^2\omega^2)}}$$

so that

$$\frac{dW}{d\omega} = \frac{1}{K'}\frac{1}{\sqrt{(1 - \omega^2)(1 - k^2\omega^2)}} \tag{58}$$

The term $d\omega/dZ$ is given by equation (A2), and the result of combining these relations into equation (57) is

$$\frac{dW}{dZ} = \frac{\sqrt{\omega}}{K'Ck} \tag{59}$$

The relation between ω and W is given by equation (A1) and the constant C by equation (A7). Hence,

$$\frac{dW}{dZ} = \sqrt{\frac{2}{1 + k}}\frac{K(k_2)}{K'}\sqrt{sn(WK' - K)} \tag{60}$$

Since $W = \psi + i$ on the boundary where $\varphi = 1$, the identity

$$sn(\psi K' + iK' - K) = \frac{1}{k\, sn(\psi K' - K)}$$

shows that when equation (60) is evaluated on this boundary the following result is obtained:

$$\left|\frac{dW}{dZ}\right|_{\varphi=1} = \sqrt{\frac{2}{k(1+k)}}\,\frac{K(k_2)}{K'(k)}\,\frac{1}{\sqrt{\left|sn(\psi K' - K, k)\right|}} \tag{61}$$

The absolute value signs are needed under the square root sign because $\psi < K/K'$ on part of the boundary (between points 6 and 5 in fig. 4(a)).

Exit Velocity at Inside Surface of Porous Duct

It follows from equations (13) and (18) that the local velocity in the porous medium is given by

$$\vec{U} = \hat{i}\,\frac{\partial\varphi}{\partial X} + \hat{j}\,\frac{\partial\varphi}{\partial Y}$$

The surface $\widehat{456}$ in figure 3(b) is at constant potential, and hence, the exit velocity from the porous medium is normal to this surface. It can be seen from the symmetry of the problem that the magnitude of the velocity is the same function of distance from the corner 5 along the boundary $\widehat{54}$ as along $\widehat{56}$; so only the former will be computed. Because $\partial\varphi/\partial X = 0$ on the boundary $\widehat{54}$, it follows that the exit velocity which is in the Y-direction is

$$V_s = \left.\frac{\partial\varphi}{\partial Y}\right|_{\varphi=1} \tag{62}$$

Since along the boundary $\widehat{54}$

$$\left.\frac{dW}{dZ}\right|_{\varphi=1} = \left[-i\,\frac{\partial\psi}{\partial Y} + \frac{\partial\varphi}{\partial Y}\right]_{\varphi=1} = \left[i\,\frac{\partial\varphi}{\partial X} + \frac{\partial\varphi}{\partial Y}\right]_{\varphi=1} = \left.\frac{\partial\varphi}{\partial Y}\right|_{\varphi=1} \tag{63}$$

it can be seen from equations (62) and (63) that

$$V_s = \left.\frac{dW}{dZ}\right|_{\varphi=1} \tag{64}$$

By using equation (61) the exit velocity distribution is found to be

$$V_s = \sqrt{\frac{2}{k(1+k)}} \frac{K(k_2)}{K'(k)} \frac{1}{\sqrt{sn(\psi K' - K, k)}} \tag{65}$$

The mapping in equation (A16b) relates ψ to X'_s so that V_s can then be found as a function of position along $\widehat{54}$.

Solution With Specified Uniform Temperature on Each Surface of Interior Duct

Equation (53) provides the dimensionless heat flux along the surface on which the wall temperature variation has been specified by equation (7a). To demonstrate the application of this solution, consider the case where one surface of the duct corresponding to side $\widehat{65}$ in figure 3(b) is at the uniform temperature t_1 while side $\widehat{54}$ is at a different uniform temperature t_2. Then in the boundary condition (37a) the function $H(L_s)$ of ψ becomes a unit step function that is equal to zero when ψ lies between 0 and K/K'(0 to $\psi_r/2$) and is equal to unity when ψ is between K/K' and $2K/K'$ ($\psi_r/2$ to ψ_r).

The coefficients B_0 and B_n given by equation (51) now become

$$B_0 = \frac{1}{\psi_r} \int_{\psi_r/2}^{\psi_r} d\psi = \frac{1}{2} \tag{66a}$$

$$B_n = \frac{2}{\psi_r} \int_{\psi_r/2}^{\psi_r} \cos\left(\frac{n\pi\psi}{\psi_r}\right) d\psi = -\frac{2}{n\pi} \sin\frac{n\pi}{2} = -\frac{2}{n\pi}(-1)^{(n-1)/2} \qquad n = 1, 3, 5, \ldots \tag{66b}$$

Therefore, equation (53) becomes

$$\frac{q_s h_r}{k_m(t_1 - t_\infty)} = \left|\frac{dW}{dZ}\right|_{\varphi=1} \left\{ 2\lambda + \lambda N H(L_s(\psi)) + \frac{N}{2}\left[\gamma_n \frac{\lambda \cosh \gamma_n + \gamma_n \sinh \gamma_n}{\lambda \sinh \gamma_n + \gamma_n \cosh \gamma_n}\right]_{n=0} \right.$$

$$\left. - \frac{2N}{\pi} \sum_{n=1,3,5,\ldots}^{\infty} \frac{(-1)^{(n-1)/2}}{n} \gamma_n \left[\frac{\lambda \cosh \gamma_n + \gamma_n \sinh \gamma_n}{\lambda \sinh \gamma_n + \gamma_n \cosh \gamma_n}\right] \cos \frac{n\pi\psi}{\psi_r} \right\}$$

$$= \left|\frac{dW}{dZ}\right|_{\varphi=1} \left\{ \lambda\left[2 + \frac{N}{2} + N H(L_s(\psi))\right] \right.$$

$$\left. - \frac{2N}{\pi} \sum_{n=1,3,5,\ldots}^{\infty} \frac{(-1)^{(n-1)/2}}{n} \gamma_n \left[\frac{\lambda \cosh \gamma_n + \gamma_n \sinh \gamma_n}{\lambda \sinh \gamma_n + \gamma_n \cosh \gamma_n}\right] \cos \frac{n\pi}{\psi_r} \psi \right\} \qquad (67)$$

For large n, equation (48) shows that $\gamma_n \sim n\pi/\psi_r$ and the n^{th} term of the series in equation (63) behaves like

$$\frac{(-1)^{(n-1)/2}}{n} \frac{n\pi}{\psi_r} \left[\frac{\lambda \cos \frac{n\pi}{\psi_r} + \frac{n\pi}{\psi_r} \sinh \frac{n\pi}{\psi_r}}{\lambda \sinh \frac{n\pi}{\psi_r} + \frac{n\pi}{\psi_r} \cosh \frac{n\pi}{\psi_r}}\right] \cos \frac{n\pi}{\psi_r} \psi \sim (-1)^{(n-1)/2} \frac{\pi}{\psi_r} \cos \frac{n\pi}{\psi_r} \psi$$

so that the formal Fourier series in equation (67) does not converge. To remedy this, we add and subtract the divergent part of the series to obtain

$$\frac{q_s h_r}{k_m(t_1 - t_\infty)} = \left|\frac{dW}{dZ}\right|_{\varphi=1} \left\{ \lambda\left[2 + \frac{N}{2} + NH(L_s(\psi))\right] - \frac{2N}{\pi}\frac{\pi}{\psi_r} \sum_{n=1,3,5,\ldots}^{\infty} (-1)^{(n-1)/2} \cos\frac{n\pi}{\psi_r}\psi \right.$$

$$\left. - \frac{2N}{\pi} \sum_{n=1,3,5,\ldots}^{\infty} \left[\frac{(-1)^{(n-1)/2}}{n} \frac{\left(\gamma_n^2 - \lambda\frac{n\pi}{\psi_r}\right)\sinh\gamma_n + \gamma_n\left(\lambda - \frac{n\pi}{\psi_r}\right)\cosh\gamma_n}{\lambda\sinh\gamma_n + \gamma_n\cosh\gamma_n} \right] \cos\frac{n\pi}{\psi_r}\psi \right\} \qquad (68)$$

The last series in equation (68) now converges, but the series

$$\sum_{n=1,3,5,\ldots}^{\infty} (-1)^{(n-1)/2}\left(\cos\frac{n\pi}{\psi_r}\psi\right) \qquad (69)$$

does not.

It is shown in appendix B that this series is the formal Fourier series for the function $(1/2)/\cos(\pi\psi/\psi_r)$. Hence, when the divergent series is replaced by the singular function which it represents, the solution becomes in its final form

$$\frac{q_s h_r}{k_m(t_1 - t_\infty)} = \left|\frac{dW}{dZ}\right|_{\varphi=1} \left\{ \lambda\left[2 + \frac{N}{2} + NH(L_s(\psi))\right] - \frac{N}{\psi_r} \frac{1}{\cos \frac{\pi\psi}{\psi_r}} \right.$$

$$\left. - \frac{2N}{\pi} \sum_{n=1,3,5,\ldots}^{\infty} \frac{(-1)^{(n-1)/2}}{n} \left[\frac{\left(\gamma_n^2 - \lambda \frac{n\pi}{\psi_r}\right)\sinh \gamma_n + \gamma_n\left(\lambda - \frac{n\pi}{\psi_r}\right)\cosh \gamma_n}{\lambda \sinh \gamma_n + \gamma_n \cosh \gamma_n} \right] \cos \frac{n\pi}{\psi_r}\psi \right\} \qquad (70)$$

The manipulations carried out above were purely formal since it is not in general proper to add and subtract divergent series or to allow them to represent functions. However, these manipulations are justified in the case of Fourier series by the use of the theory of distributions. This justification is given, for example, in reference 5.

For the special case when the imposed surface temperature is uniform around the entire duct interior, the parameter N in equation (70) is zero. Then equation (70) simplifies to

$$\frac{q_s h_r}{k_m(t_1 - t_\infty)} = \left|\frac{dW}{dZ}\right|_{\varphi=1} 2\lambda$$

Therefore, equation (64) shows that for the uniform surface temperature case,

$$\frac{q_s h_r}{2\lambda k_m(t_1 - t_\infty)} = V_s \qquad (71)$$

Temperature Distribution for Imposed Uniform Heat Flux

When the imposed heat flux on the inner surface of the duct is uniform, equation (10)

shows that $M = 0$. Consequently, equation (55) becomes in this case

$$E_0 = \frac{1}{\psi_r} \int_0^{\psi_r} \left| \frac{dZ}{dW} \right|_{\varphi=1} d\psi \tag{72a}$$

$$E_n = \frac{2}{\psi_r} \int_0^{\psi_r} \left| \frac{dZ}{dW} \right|_{\varphi=1} \cos\left(\frac{n\pi\psi}{\psi_r}\right) d\psi \qquad \text{for } n = 1, 2, 3, \ldots \tag{72b}$$

In view of the symmetry of the duct, it can be seen that the function $\left|dZ/dW\right|_{\varphi=1}$ (which is the reciprocal of the exit velocity from the porous material) is an even function of ψ with respect to the point $\psi_r/2$. The quantity $\cos(n\pi\psi/\psi_r)$, however, is an odd function with respect to the point $\psi_r/2$ for odd values of n. Hence, $E_n = 0$ for odd values of n. Therefore, upon removing the term containing E_0 from the sum, the solution for the surface temperature distribution given by equation (56) can, in this case, be written as

$$\frac{(t_s - t_\infty)k_m}{h_r q_s} = \frac{E_0}{2\lambda} + \sum_{n=1,3,5,\ldots}^{\infty} E_n \left[\frac{\lambda \sinh \gamma_n + \gamma_n \cosh \gamma_n}{\left(\lambda^2 + \gamma_n^2\right) \sinh \gamma_n + 2\lambda\gamma_n \cosh \gamma_n} \right] \cos\left(\frac{n\pi}{\psi_r}\psi\right) \tag{73}$$

DISCUSSION

A general analytical solution was obtained for the heat-transfer behavior in a two-dimensional porous medium with coolant being forced through it. The application of the solution was demonstrated by examining the heat transfer in a square duct with porous cooled walls. Coolant from a reservoir which surrounds the duct is being forced through the walls to the duct interior.

In the general analysis, two of the boundaries of the porous region are at constant pressure while the other two have no flow across them. As a result of these conditions the porous region occupies a rectangle in the velocity potential plane. The energy equation for the temperature distribution in the medium is a separable equation when expressed in terms of the independent variables of the potential plane. General solutions independent of the specific geometry can then be found in this rectangular region. Solutions of this type were obtained for both the case of an arbitrary specified temperature

and the case of a specified heat flux on the porous material boundary through which the coolant exits. The general solutions can then be carried from the rectangular region into specific physical geometries by conformal mapping.

Some typical results for the porous cooled square duct which was analyzed in detail will now be discussed. First, consider the coolant exit velocity along the duct interior surface. This is given by equation (65) as a function of ψ, which is related to the physical coordinate by equation (A16b). The parameter in equation (65) is k (which also determines k_1 and k_2). The constant k is related to the geometric quantity A by equation (A8), where A is the ratio of half-width of the outside of the duct to the wall thickness.

The dimensionless exit velocity and duct cross sections for three values of A are shown in figure 5. For one-dimensional flow through a plane slab the dimensionless velocity $v_s \mu h_r / \kappa(p_0 - p_s)$ is unity and the present results approach this limit in the central region of the duct side as A becomes large. The velocity is high near the duct interior corner because there is less flow resistance in this region as a result of the larger outside surface area and consequently larger cross sectional area for the flow to pass through. At the duct interior corner the velocity becomes infinite. As evidenced by the deviation of the curve for A = 2.5 from unity the two-dimensional effects are confined to the region within one duct wall thickness of the interior corner.

Next, consider the heat transfer behavior when there is a specified temperature dis-

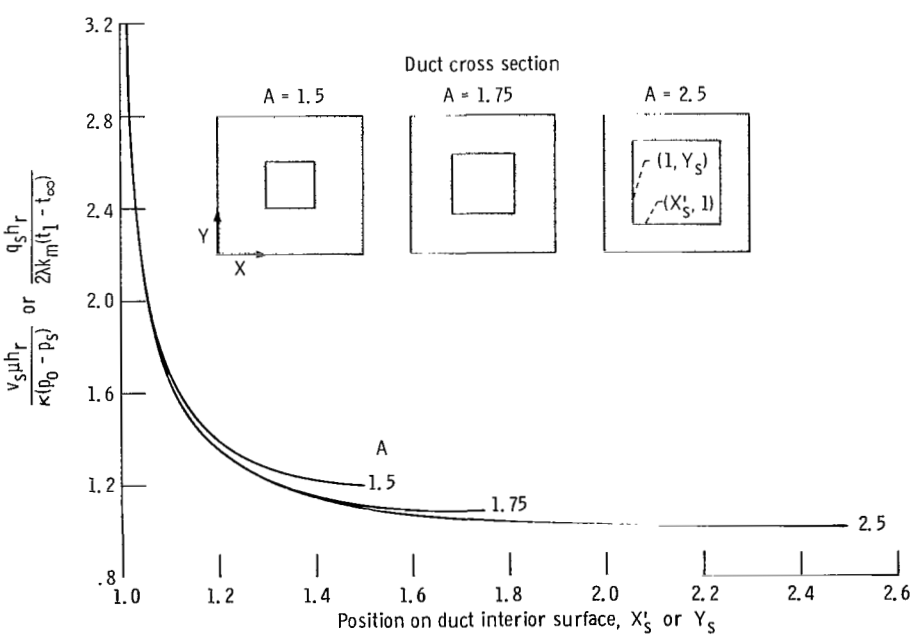

Figure 5. - Dimensionless fluid exit velocity or dimensionless heat flux when surface is at uniform temperature.

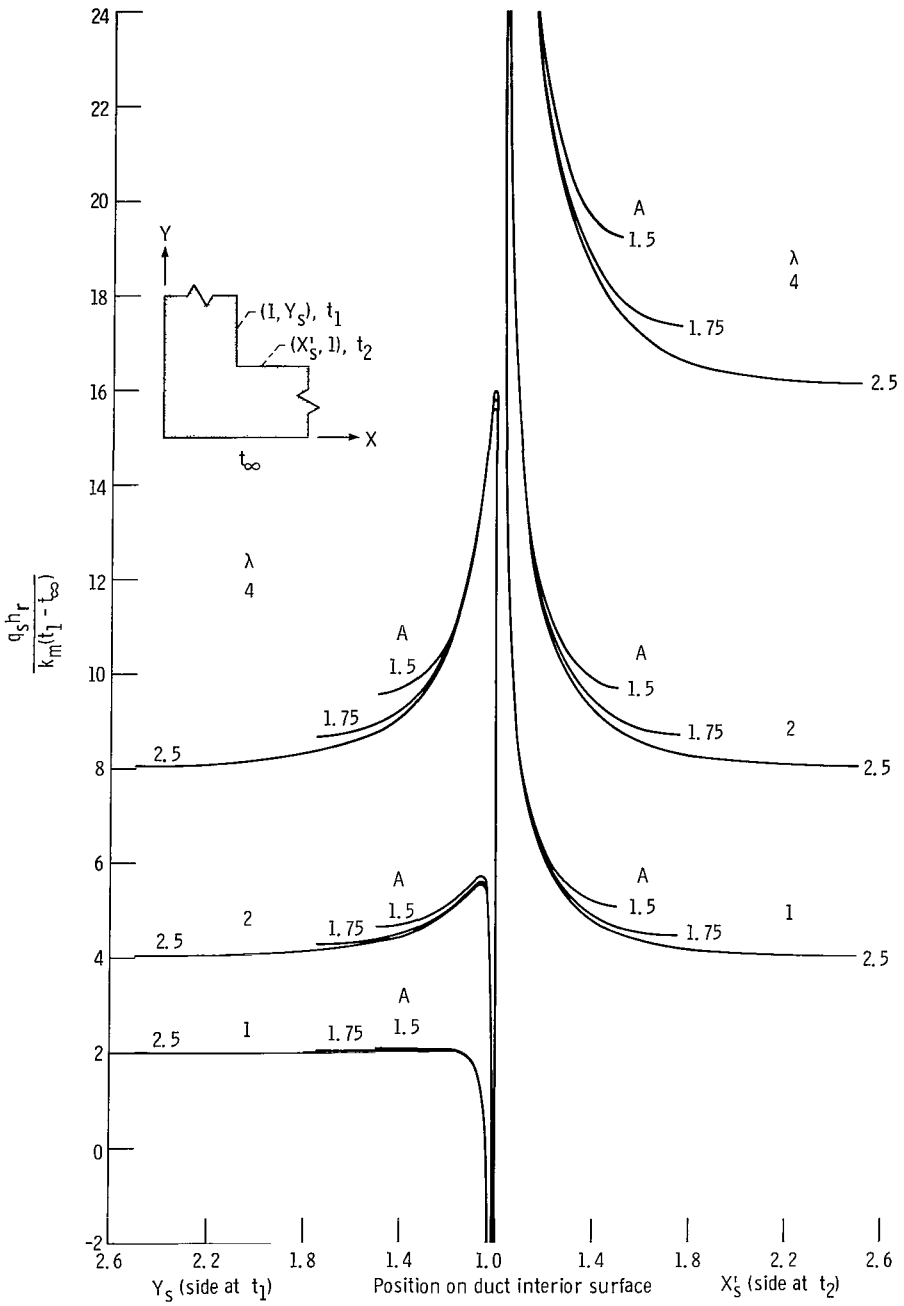

Figure 6. - Heat flux along duct interior surface for adjacent sides each at different uniform temperature, $N = (t_2 - t_1)/(t_1 - t_\infty) = 1$.

tribution on the inside of the duct. Specifically, it is desired to know for a given temperature what heat flux occurs at the surface. For a uniform surface temperature, equation (71) shows that the dimensionless heat flux $q_s h_r/2\lambda k_m(t_1 - t_\infty)$ is equal to the fluid exit velocity. Hence, the ordinate of figure 5 can also be labeled as the dimensionless heat flux for the uniform surface temperature case.

Equation (70) provides results for the situation where adjacent sides of the duct interior are at different uniform temperatures t_1 and t_2. For the set of numerical results that will be given, the parameter $N = (t_2 - t_1)/(t_1 - t_\infty)$ was set equal to unity. In figure 6, for each value of λ there are three curves corresponding to the geometries $A = 1.5$, 1.75, and 2.5. The parameter $\lambda = (\rho C_p/2k_m)\left[\kappa(p_o - p_s)/\mu\right]$ regulates the general level of the curves. A large value of $p_o - p_s$ and, hence, large λ, is associated with a large flow; therefore, the heat flux imposed at the surface is increased for the same surface temperature. As in the case of a uniform temperature all around the interior of the duct, the resulting surface heat flux along each duct side rises toward the corner because of the larger flow velocity there. However, very close to the corner there is a superimposed local heat conduction effect that alters this trend. Heat flows locally by conduction from the side at high temperature t_2 to the side at low temperature t_1, where it must be carried away from the surface in order to maintain the surface temperature discontinuity. This means that local surface cooling must be provided on the low temperature boundary adjacent to the temperature step. This is the region of negative heat flux in figure 6.

Figure 7 gives the surface temperature distribution for the situation where there is a uniform heat flux imposed along the entire interior surface of the duct. This solution was given by equation (73) and involves the two parameters λ and A. The parameter A occurs because it determines the parameter k through the relation in equation (A8) and k then fixes $\psi_r = 2K(k)/K'(k)$. Results are given for the three values of A shown in figure 7 for each of three values of λ.

Since the surface heat flux is uniform, the surface temperature is lowest at the corner where according to figure 5 the fluid velocity is high. A larger value of λ corresponds to a larger pressure drop and, hence, to greater flow through the porous material. Consequently, the lowest surface temperatures correspond to the largest values of λ.

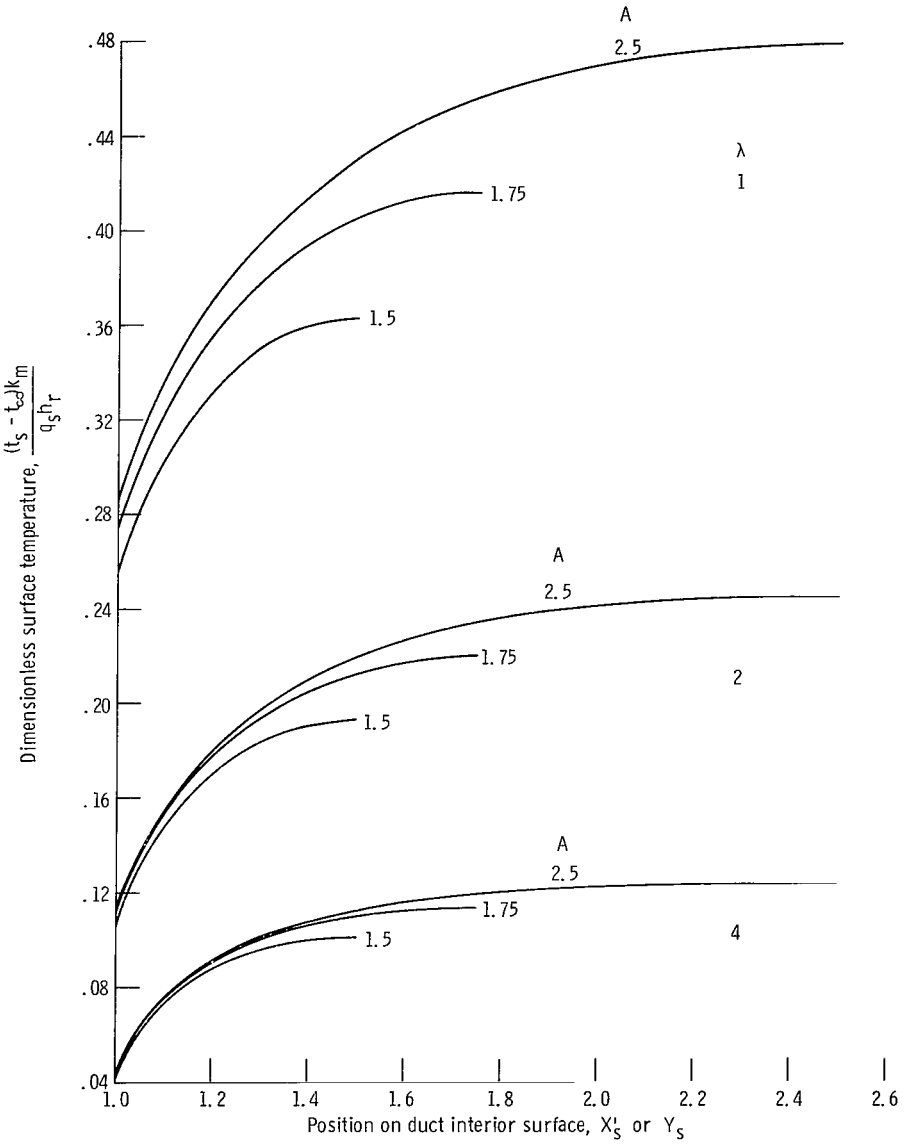

Figure 7. - Surface temperature distribution for imposed uniform heat flux along duct interior boundary.

CONCLUDING REMARKS

An analytical technique has been developed for determining the heat-transfer behavior for a finite two-dimensional porous cooled medium. It was shown that, for the boundary conditions imposed herein, every porous material configuration maps into a rectangular region in the velocity potential plane. The energy equation is transformed into this plane and a general solution obtained. This solution can be mapped into a physical shape by using the conformal mapping between the rectangle and the physical plane.

As a demonstration of the method, heat transfer results were obtained for a square duct with porous cooled walls. Coolant is being forced through the walls into the duct interior. The two-dimensional effects along the duct interior surface were found to be confined to within approximately one wall thickness of the duct interior corner.

Lewis Research Center,
National Aeronautics and Space Administration,
Cleveland, Ohio, July 17, 1970,
129-01.

APPENDIX A

MAPPING OF QUARTER OF DUCT INTO RECTANGLE OF POTENTIAL PLANE

In order to relate the solution obtained in the potential plane (W-plane) to the physical geometry (Z-plane), the conformal mapping between these two regions must be found. The appropriate regions for this geometry are shown in the physical and potential planes in figures 3(b) and 4(a). First, it will be convenient to express this mapping in terms of the variables in the intermediate ω-plane shown in figure 4(b). Here the region occupies the upper half plane with the boundary along the real (ξ) axis. Then to aid in some of the mathematical manipulation it will be convenient to transform the results into the u-plane shown in figure 4(c). In this plane the porous region occupies the entire plane with the boundary of the porous region lying along the two cuts on the real axis shown in the figure.

The mapping that transforms the W-plane into the ω-plane in the manner shown by figures 4(a) and (b) is given in reference 6 as

$$\omega = \mathrm{sn}(WK' - K) \tag{A1}$$

The mapping that transforms the Z-plane into the ω-plane in the manner shown by figures 3(b) and 4(b) is found by use of the Schwarz-Christoffel transformation to be determined by

$$\frac{dZ}{d\omega} = \frac{C}{\sqrt{\omega(\omega^2 - 1)\left(\omega^2 - \frac{1}{k^2}\right)}} \tag{A2}$$

or

$$Z - C_1 = -Ck \int \frac{d\omega}{\sqrt{\omega(1 - \omega^2)(1 - k^2\omega^2)}} \tag{A3}$$

where C_1 is a constant of integration.

The integral in equation (A3) is of the type treated by relation 596.00 on page 268 of reference 7. To simplify the integrals, the transformation

$$\omega = \frac{1}{2k}\left(u + \sqrt{u^2 - 4k}\right) \tag{A4}$$

is used. As shown in reference 7, equation (A3) then transforms into

$$Z - C_1 = -\frac{Ck}{2}\left\{\int \frac{du}{\sqrt{(u - 2\sqrt{k})\left[u^2 - (1 + k)^2\right]}} - \int \frac{du}{\sqrt{(u + 2\sqrt{k})\left[u^2 - (1 + k)^2\right]}}\right\} \tag{A5}$$

The transformation (A4) relates the regions in the ω- and u-planes as shown in figures 4(b) and (c).

The origin of the Z-plane is at point 2, which corresponds to the point $\infty - i\epsilon$ in the u-plane. By integrating from point 2 to any point in the u-plane, equation (A5) then provides the following relation between the position in the physical plane and the parametric variable u:

$$Z = -\frac{Ck}{2}\left\{\int_{\infty - i\epsilon}^{u} \frac{du}{\sqrt{(u - 2\sqrt{k})\left[u^2 - (1 + k)^2\right]}} - \int_{\infty - i\epsilon}^{u} \frac{du}{\sqrt{(u + 2\sqrt{k})\left[u^2 - (1 + k)^2\right]}}\right\} \tag{A6}$$

The constant C can be obtained by noting that in figure 3(b) $Z_4 - Z_3 = i$. Equation A(6) is then integrated along the branch cut in figure 4(c) from point 3 at $u = 1 + k - i\epsilon$ to $u = 2\sqrt{k}$ and then from $u = 2\sqrt{k}$ to $u = 1 + k + i\epsilon$. Equating the result to i gives after some simplification

$$i = \frac{Ck}{2} 2i \int_{2\sqrt{k}}^{1+k} \frac{d\alpha}{\sqrt{(\alpha - 2\sqrt{k})\left[(k + 1)^2 - \alpha^2\right]}}$$

By use of relation 236.00 in reference 7, the integral can be converted to an elliptic integral. This shows that the constant C is related to the parameter k by

$$C = \frac{1}{k\sqrt{\frac{2}{1 + k}}\, K\left(\frac{1 - \sqrt{k}}{\sqrt{2(1 + k)}}\right)} \tag{A7}$$

The quantity k will now be expressed in terms of a physical quantity. The only geometric parameter for the square duct configuration is the dimensionless half-width A shown in figure 3(b) and equal to $Z_3 - Z_2$. Thus, to obtain an expression for A,

equation (A6) is evaluated between points 2 and 3 along the branch cut in figure 4(c). This yields

$$A = -\frac{Ck}{2}\left\{\int_{\infty}^{1+k} \frac{d\alpha}{\sqrt{(\alpha - 2\sqrt{k})\left[\alpha^2 - (k+1)^2\right]}} + \int_{\infty}^{1+k} \frac{d\alpha}{\sqrt{(\alpha + 2\sqrt{k})\left[\alpha^2 - (k+1)^2\right]}}\right\}$$

By use of relation 238.00 in reference 7, these integrals are expressed as elliptic integrals, and the constant C is eliminated by using equation (A7). When this is done, we obtain the following relation between the physical quantity A and the mapping parameter k:

$$A = \frac{1}{2K(k_2)}\left[K(k_1) + K(k_2)\right] \tag{A8}$$

where

$$k_1 = \frac{1 + \sqrt{k}}{\sqrt{2(1+k)}} \qquad k_2 = \frac{1 - \sqrt{k}}{\sqrt{2(1+k)}}$$

In order to complete the solution to the problem, it is necessary to find the relations between the values of ψ along the boundary $\varphi = 1$ and the physical Z-plane.

For convenience let the coordinates between points 5 and 4 be called X'_s, Y'_s while those from 5 to 6 are X_s, Y_s (fig. 3(b)). Note that Z_5 is at $1 + i$ and evaluate equation (A6) along the branch cuts in figure 4(c) from point 5 to an arbitrary point between either 5 and 4 or 5 and 6. This yields

$$Z'_s = 1 + i + \frac{kC}{2}\left\{\int_{\alpha}^{\infty} \frac{d\alpha}{\sqrt{(\alpha - 2\sqrt{k})\left[\alpha^2 - (k+1)^2\right]}} - \int_{\alpha}^{\infty} \frac{d\alpha}{\sqrt{(\alpha + 2\sqrt{k})\left[\alpha^2 - (k+1)^2\right]}}\right\}$$

$$1 + k \le \alpha \le \infty \tag{A9a}$$

$$Z_s = 1 + i + \frac{kC}{2} i \left\{ \int_{-\alpha}^{\infty} \frac{d\alpha}{\sqrt{(\alpha - 2\sqrt{k})\left[\alpha^2 - (k+1)^2\right]}} - \int_{-\alpha}^{\infty} \frac{d\alpha}{\sqrt{(\alpha + 2\sqrt{k})\left[\alpha^2 - (k+1)^2\right]}} \right\}$$

$$-\infty \leq \alpha \leq -(1+k) \qquad \text{(A9b)}$$

By use of 238.00 in reference 7 the integrals are converted to elliptic integrals, the constant C is substituted from equation (A7), and the real and imaginary parts are taken to yield

$$X_s = 1$$

$$Y_s = 1 + \frac{1}{2K(k_2)} \left[F\left(\sin^{-1} \sqrt{\frac{2(1+k)}{-\alpha + (1+k)}}, k_1 \right) - F\left(\sin^{-1} \sqrt{\frac{2(1+k)}{-\alpha + (1+k)}}, k_2 \right) \right] \quad -\infty \leq \alpha \leq -(1+k) \qquad \text{(A10a)}$$

$$X_s' = 1 + \frac{1}{2K(k_2)} \left[F\left(\sin^{-1} \sqrt{\frac{2(1+k)}{\alpha + (1+k)}}, k_1 \right) - F\left(\sin^{-1} \sqrt{\frac{2(1+k)}{\alpha + (1+k)}}, k_2 \right) \right] \quad 1 + k \leq \alpha \leq \infty \qquad \text{(A10b)}$$

$$Y_s' = 1$$

Now it follows from equation (A4) that $2k\omega - u = \sqrt{u^2 - 4k}$. Square both sides and solve for u to obtain

$$u = k\omega + \frac{1}{\omega} \qquad \text{(A11)}$$

In the ranges $1 + k \leq \alpha \leq \infty$ and $-\infty \leq \alpha \leq -(1 + k)$, for which equation (A10) applies, the points are on the real axis of both the u- and ω-planes so that equation (A11) gives

$$\alpha = k\xi + \frac{1}{\xi} \tag{A12}$$

This is substituted into equation (A10) to give

$$\left.\begin{aligned} X_s &= 1 \\ Y_s &= 1 + \frac{1}{2K(k_2)}\left[F\left(\sin^{-1}\sqrt{\frac{2(1+k)}{-k\xi - \frac{1}{\xi} + 1 + k}},\ k_1\right)\right. \\ &\qquad \left. -F\left(\sin^{-1}\sqrt{\frac{2(1+k)}{-k\xi - \frac{1}{\xi} + 1 + k}},\ k_2\right)\right] \end{aligned}\right\} -\infty \leq \xi \leq -\frac{1}{k} \tag{A13a}$$

$$\left.\begin{aligned} X'_s &= 1 + \frac{1}{2K(k_2)}\left[F\left(\sin^{-1}\sqrt{\frac{2(1+k)}{k\xi + \frac{1}{\xi} + 1 + k}},\ k_1\right)\right. \\ &\qquad \left. -F\left(\sin^{-1}\sqrt{\frac{2(1+k)}{k\xi + \frac{1}{\xi} + 1 + k}},\ k_2\right)\right] \\ Y'_s &= 1 \end{aligned}\right\} \frac{1}{k} \leq \xi \leq \infty \tag{A13b}$$

Equation (A1) relates the ω- and W-planes and can be used to make the final transformation of equation (A13) and relate X_s, Y_s and X'_s, Y'_s to ψ. For X_s, Y_s the coordinates are between points 6 and 5, and from figure 4(a), $W = \psi + i$ where $0 \leq \psi \leq K/K'$. Then

$$\xi = sn(\psi K' + iK' - K)$$

which gives

$$\xi = -\frac{1}{k}\frac{1}{sn(K - \psi K')} \qquad \begin{cases} 0 \le \psi \le \dfrac{K}{K'} \\ -\infty \le \xi \le -\dfrac{1}{k} \end{cases} \tag{A14a}$$

Similarly, between points 5 and 4

$$\xi = \frac{1}{k}\frac{1}{sn(\psi K' - K)} \qquad \begin{cases} \dfrac{K}{K'} \le \psi \le 2\dfrac{K}{K'} \\ \dfrac{1}{k} \le \xi \le \infty \end{cases} \tag{A14b}$$

Equations (A14) are used in (A13) to eliminate ξ. Note that

$$\left[\frac{2(1+k)}{\pm k\xi \pm \frac{1}{\xi} + 1 + k}\right]^{1/2} = \left[\frac{2}{\pm\xi}\frac{1+k}{\left(1 \pm \frac{1}{\xi}\right)\left(k \pm \frac{1}{\xi}\right)}\right]^{1/2}$$

Substitute either (A14a) or (A14b) and define Ω as

$$\Omega \equiv \left\{\frac{2(1+k)\left|sn(\psi K' - K, k)\right|}{\left[1 + k\left|sn(\psi K' - K, k)\right|\right]\left[1 + \left|sn(\psi K' - K, k)\right|\right]}\right\}^{1/2} \tag{A15}$$

Then equations (A13) become

$$\left.\begin{aligned} X_s &= 1 \\ Y_s &= 1 + \frac{1}{2K(k_2)}\left[sn^{-1}(\Omega, k_1) - sn^{-1}(\Omega, k_2)\right] \end{aligned}\right\} \quad 0 \le \psi \le \frac{K}{K'} \tag{A16a}$$

$$\left.\begin{aligned} X'_s &= 1 + \frac{1}{2K(k_2)}\left[sn^{-1}(\Omega, k_1) - sn^{-1}(\Omega, k_2)\right] \\ Y'_s &= 1 \end{aligned}\right\} \frac{K}{K'} \leq \psi \leq \frac{2K}{K'} \qquad \text{(A16b)}$$

If we cross multiply,

$$(z - e^{-aT})y(z) = k(z - 1)x(z)$$

divide by z,

$$\left(1 - \frac{e^{-aT}}{z}\right)y(z) = k\left(1 - \frac{1}{z}\right)x(z)$$

transform to the discrete time domain, remembering that $(1/z)y_n = y_{n-1}$

$$y_n - e^{-aT}y_{n-1} = k(x_n - x_{n-1})$$

and rearranging, the final form of the difference equation is obtained:

$$y_n = e^{-aT}y_{n-1} + k(x_n - x_{n-1})$$

At the sampling points, the difference equation is the exact solution for the response of the equivalent analog system to a stair-step function input. Therefore, the solution does not become numerically unstable for large sampling intervals. However, the output of the system will be realistic only if the sampling is done frequently enough to result in a stair-step waveform which is a good approximation of the original continuous input waveform.

For comparison, the equations for the above filter using numerical integration (fourth-order Adams-Bashford) are:

$$y_n = y_{n-1} + \frac{T}{24}\left(55\dot{y}_n - 59\dot{y}_{n-1} + 37\dot{y}_{n-2} - 9\dot{y}_{n-3}\right)$$

$$\dot{y}_n = -ay_n + kx_n$$

The computation efficiency of the difference equation is obviously better than that of the numerical integration technique. Also, this numerical integration method becomes numerically unstable for large sampling intervals, as confirmed during the investigation.

Difference equations were used to simulate the aircraft control and automatic stabilization systems, to replace the analog autopilot with a digital version, and to generate the turbulent wind components.

The aircraft control system simulator consists of a throttle servo with engine lag and an elevator servo with an elevator surface lag. Both of these servos have the same general form, a second-order transfer function with 0.7 critical damping in series with a first-order low pass filter. The form of the total transfer function and the corresponding difference equation are shown in section 7 of table 8.

The washout filter in the stability augmentation system discussed above is simulated by the difference equation of section 1 in table 8.

$$\frac{1}{1+\exp\left\{-\left[1+iW-ic\right]\frac{\pi}{\psi_r}\right\}}-\frac{1}{1+\exp\left\{-\left[1+iW+ic\right]\frac{\pi}{\psi_r}\right\}}$$

$$=2i\sum_{n=0}^{\infty}(-1)^n\, e^{-(n\pi/\psi_r)(1-\varphi)}\, e^{-(n\pi i/\psi_r)\psi}\sin\frac{n\pi c}{\psi_r}\qquad \text{for}\quad \varphi<1 \qquad \text{(B2)}$$

Upon combining the two fractions on the left side of equation (B2) and collecting terms, we find

$$\frac{1}{1+\exp\left\{-\left[1+iW-ic\right]\frac{\pi}{\psi_r}\right\}}-\frac{1}{1+\exp\left\{-\left[1+iW+ic\right]\frac{\pi}{\psi_r}\right\}}$$

$$=-i\sin\frac{\pi c}{\psi_r}\Bigg/\left\{\cos\left[\frac{\pi}{\psi_r}(\psi+i\varphi-i)\right]+\cos\frac{\pi c}{\psi_r}\right\}$$

Hence, equation (B2) becomes

$$-\frac{1}{2}\,\frac{\sin\frac{\pi c}{\psi_r}}{\cos\left[\frac{\pi}{\psi_r}(\psi+i\varphi-i)\right]+\cos\frac{\pi c}{\psi_r}}$$

$$=\sum_{n=0}^{\infty}(-1)^n\, e^{-(n\pi/\psi_r)(1-\varphi)}\, e^{-(n\pi i\psi)/\psi_r}\sin\left(\frac{n\pi c}{\psi_r}\right)\qquad \text{for}\quad \varphi<1$$

Or upon taking real parts,

$$-\frac{1}{2}\,Re\left\{\frac{\sin\frac{\pi c}{\psi_r}}{\cos\frac{\pi c}{\psi_r}+\cos\left[\frac{\pi}{\psi_r}(\psi+i\varphi-i)\right]}\right\}$$

$$=\sum_{n=0}^{\infty}(-1)^n\,e^{-(n\pi/\psi_r)(1-\varphi)}\,\sin\frac{n\pi c}{\psi_r}\cos\frac{n\pi\psi}{\psi_r}\qquad\text{for}\quad\varphi<1$$

Upon taking the limit $\varphi \to 1$, we find that relation (B1) holds. Of course this limit must be taken in the sense of distributions, in which case the interchange of the limit associated with the summation and the limit associated with φ is justified.

REFERENCES

1. Siegel, Robert; and Goldstein, Marvin E.: Analytical Method for Steady State Heat Transfer in Two Dimensional Porous Media. NASA TN D-5878, 1970.
2. Barfield, W. D.: Numerical Method for Generating Orthogonal Curvilinear Meshes. J. Computational Phys., vol. 5, no. 1, Feb. 1970, pp. 23-33.
3. Boussinesq, M. J.: Calcu du Pouvoir Refroidissand des Courants Fluides. J. Math. Pure et Appl., I, 1905, pp. 285-332.
4. Churchill, Ruel V.: Complex Variables and Applications. Second ed., McGraw-Hill Book Co., Inc., 1960.
5. Lighthill, M. J.: Introduction to Fourier Analysis and Generalized Functions. Cambridge Univ., Press, 1964.
6. Moretti, Gino: Functions of a Complex Variable. Prentice-Hall, Inc., 1964, p. 359.
7. Byrd, Paul F.; and Friedmann, Morris D.: Handbook of Elliptic Integrals for Engineers and Physicists. Springer-Verlag, 1954.

NASA-Langley, 1970 —— 33 E-5677

"The aeronautical and space activities of the United States shall be conducted so as to contribute . . . to the expansion of human knowledge of phenomena in the atmosphere and space. The Administration shall provide for the widest practicable and appropriate dissemination of information concerning its activities and the results thereof."

—NATIONAL AERONAUTICS AND SPACE ACT OF 1958

NASA SCIENTIFIC AND TECHNICAL PUBLICATIONS

TECHNICAL REPORTS: Scientific and technical information considered important, complete, and a lasting contribution to existing knowledge.

TECHNICAL NOTES: Information less broad in scope but nevertheless of importance as a contribution to existing knowledge.

TECHNICAL MEMORANDUMS: Information receiving limited distribution because of preliminary data, security classification, or other reasons.

CONTRACTOR REPORTS: Scientific and technical information generated under a NASA contract or grant and considered an important contribution to existing knowledge.

TECHNICAL TRANSLATIONS: Information published in a foreign language considered to merit NASA distribution in English.

SPECIAL PUBLICATIONS: Information derived from or of value to NASA activities. Publications include conference proceedings, monographs, data compilations, handbooks, sourcebooks, and special bibliographies.

TECHNOLOGY UTILIZATION PUBLICATIONS: Information on technology used by NASA that may be of particular interest in commercial and other non-aerospace applications. Publications include Tech Briefs, Technology Utilization Reports and Notes, and Technology Surveys.

Details on the availability of these publications may be obtained from:

SCIENTIFIC AND TECHNICAL INFORMATION DIVISION

NATIONAL AERONAUTICS AND SPACE ADMINISTRATION

Washington, D.C. 20546